Algebraic decay and fluctuations of the decay exponent in Hamiltonian systems

Ying-Cheng Lai
Laboratory for Plasma Research, University of Maryland, College Park, Maryland 20742
and Department of Physics and Astronomy, University of Maryland, College Park, Maryland 20742

Mingzhou Ding
Center for Complex Systems, Florida Atlantic University, Boca Raton, Florida 33431
and Department of Mathematics, Florida Atlantic University, Boca Raton, Florida 33431

Celso Grebogi
Laboratory For Plasma Research, University of Maryland, College Park, Maryland 20742;
Department of Mathematics, University of Maryland, College Park, Maryland 20742;
and Institute for Physical Science and Technology, University of Maryland, College Park, Maryland 20742

Reinhold Blümel
Department of Physics and Astronomy, University of Delaware, Newark, Delaware 19716
(Received 13 May 1992)

Particle-decay processes in a nonhyperbolic Hamiltonian system are typically characterized by algebraic laws. That is, for a fixed set of parameter values, if one initializes a particle in a chaotic region near some Kol'mogorov-Arnol'd-Moser (KAM) tori, the probability for this particle to remain in the region at time t decays with time algebraically: $P(t)\sim t^{-z}$, where z is the decay exponent. As a system parameter varies, the numerically calculated exponent z exhibits rather large fluctuations. In this paper we examine the dynamical origin of such fluctuations using a model system which exhibits unbounded chaotic dynamics (i.e., chaotic scattering). Our results indicate that the fluctuating behavior of z, as a function of the parameter, can be attributed to the breakup of KAM surfaces in phase space. A particularly interesting finding is that, when the outermost KAM surfaces enclosing some central island transform from absolute barriers to partial barriers (Cantori), as the parameter varies, the survival probability $P(t)$ displays two different regions of scaling behavior with different decay exponents. The time scale where this crossover takes place is found to coincide with the typical time for a particle to penetrate the newly created Cantori.

PACS number(s): 05.45.+b

I. INTRODUCTION

Hamiltonian systems arise in many situations of physical interest and can exhibit a variety of phase-space structures and dynamical behaviors. The simplest among them are integrable systems in which the entire phase space is filled with families of invariant Kol'mogorov-Arnol'd-Moser (KAM) tori giving rise to regular dynamics. In contrast, there is another extreme situation consisting of systems that are completely chaotic. In this case the invariant set in phase space often forms a single component on which the dynamics is ergodic and displays sensitive dependence on initial conditions. Examples of this latter case include the Sinai billiard system, the Bunimovich stadium, and the Arnol'd-cat map. Most Hamiltonian systems encountered in practice, however, belong to the category lying somewhere between the two extreme situations. In such systems there is typically a mixture of regular motion on KAM tori (or surfaces) and chaotic motion between these tori. One interesting issue that has been addressed in the past concerns the impact of the presence of KAM surfaces on particle motion in the nearby chaotic regions. In this regard, one generally observes that if a particle is initialized in a chaotic region near some KAM surface, then the particle wanders close to that surface for a long time. This effect is called the "stickiness" effect of the KAM surfaces. The origin of this stickiness effect can be understood by the following observation. Take two nearby points on a given KAM torus and observe their evolution. What one typically finds is that the distance between the two points hardly changes with time. This means that the Lyapunov exponents in the directions along the KAM surface are zero (i.e., the motion is quasiperiodic). On the other hand, the symplectic nature of Hamiltonian dynamics implies that the Lyapunov spectrum is organized in pairs of exponents with equal value but opposite signs. Hence an orbit on a KAM surface has zero Lyapunov exponents in directions both along and perpendicular to the surface (at least for two-dimensional maps). (Such systems with KAM surfaces are nonhyperbolic.) Now consider a particle initialized in the chaotic region. Due to ergodicity, this particle will come arbitrarily close to some KAM surface bordering the chaotic region. When this occurs, the effective Lyapunov exponents will be very small, leading to slow divergence of the particle trajectory from the

KAM surface, thereby causing the stickiness effect observed above.

The consequences of the stickiness effect on the particle transport have been numerically investigated for both two- and higher-dimensional area-preserving maps [1–5]. In what follows we review some of the main results of such studies for two-dimensional maps [1–3]. Consider a situation where the phase space is composed of a central island region bounded by some outermost KAM surfaces and a region of chaotic motion outside these KAM surfaces. Imagine that we surround the outermost KAM surfaces by a large circle situated in the chaotic region. We then place a large number of initial conditions in some small chaotic region located between the outermost KAM surface and the large circle. If the particle crosses to the outside of the large circle we regard the particle as having escaped the region containing the central island. Let $N(t)$ denote the number of particles that have not yet escaped at time t, then $N(t)$ vs t is roughly fit by an overall algebraic decay law for large t,

$$N(t) \sim t^{-z} , \tag{1}$$

where z is the decay exponent with a value estimated around 1.2–1.5 [1,2]. [Note that the survival probability $P(t)$ for an initial condition is proportional to $N(t)$.] Similar algebraic decay laws with characteristically larger decay exponents are also found in four- and six-dimensional symplectic maps with KAM surfaces [5]. It is further conjectured that this behavior is true for systems of even higher dimensionality [5]. In the light of such numerical evidence, the algebraic decay law Eq. (1), as opposed to the more rapid exponential decay exhibited by hyperbolic systems, is thought to be characteristic of the stickiness effect of the KAM surfaces. (It should be pointed out, however, that chaotic systems with no KAM surfaces may also exhibit algebraic decay behavior reflecting long-term correlation among orbits. One example of such systems is the Bunimovich stadium mentioned earlier in which the dynamics is completely chaotic. The origin of the long-term correlation in this system is considered to be due to the existence of a certain infinite class of neutrally stable periodic orbits in the phase space [6,7].) Theoretical models [8,9] have been proposed to explain the numerically observed algebraic decay law Eq. (1). A fundamental assumption of these models is that a particle in phase space executes a random walk between families of self-similar chains of islands. Such models in general yield an algebraic relationship between $N(t)$ and t, with the value of the decay exponent depending on the number of self-similar families of islands included in the calculation.

In many situations of interest the Hamiltonian system under investigation depends on some control parameters of the system. An important problem, therefore, is to discover what qualitative changes can happen to the system as a single scalar parameter is continuously varied and how such changes are manifested through experimentally observable quantities. In the context of this paper, the systems of particular interest are those that are nonhyperbolic at one set of parameter values and hyperbolic at another set of parameter values. In such systems the particle decay process changes its character from algebraic to exponential with the smooth variation of a parameter. Our main interest in this paper is to investigate the mechanism underlying the change of the decay exponent. Some consideration along this direction was given by Grassberger and Kantz [3] where they examined the deviation of the calculated Lyapunov exponent from its true value. Their calculation showed an algebraic deviation as a function of time. They attributed such behavior to the stickiness effect of the KAM surfaces. They further computed the parameter dependence of the decay exponents and found substantial fluctuations in the exponent. However, no detailed reasoning was furnished in their paper to explain the phenomenon.

In this paper we study the decay exponent z as defined in Eq. (1) and its dependence on some control parameter. Using a mode system which exhibits unbounded chaotic dynamics (i.e., chaotic scattering) we show that the exponent z fluctuates substantially as a function of the control parameter. The origin of such fluctuations can be understood in terms of the continual process of KAM surface breakup in phase space. To heuristically illustrate our theoretical consideration we utilize a two-dimensional model in which phase space is assumed to have a central island encircled by some outermost KAM surface and a chaotic region outside the KAM surface containing smaller island chains. For particles initialized in the chaotic region, their escape process will take place on a wide range of time scales. More specifically, based on the respective dynamical behavior in phase space, the entire time interval can be divided into two subintervals, namely, $0 < t < t_1$ and $t > t_i$. For those particles that escape before $t = t_1$, it is likely that their motions are not impacted by any KAM surfaces along their trajectories. Thus the portion of the $N(t)$ vs t curve for $t < t_1$ is exponential rather than algebraic. (In other words, these orbits only experience the hyperbolic component of the invariant set.) For the particles which stay longer than $t = t_1$ in the region, their corresponding trajectories may spend substantial amount of time near some accessible KAM surfaces. Hence the curve $N(t)$ vs t is algebraic for $t > t_1$. From an observational point of view, the more dominant the island chains are in the chaotic region, the more time the particles spend near them, thus slower is the escape process. "Slower" here is quantified by smaller decay exponent z in Eq. (1). This intuition is consistent with the theoretical picture proposed in Ref. [9] where the value of the calculated decay exponent decreases as the number of island chains included in the calculation increases. As a system parameter varies, KAM islands are destroyed continuously so that the area occupied by the regular components in the chaotic region decreases. (It is also possible that entire island chains are destroyed in this process.) This picture suggests that the decay exponent z will increase as the system parameter increases.

The above argument holds true up to the point where some KAM surfaces undergo transformations from being absolute barriers to partial barriers called Cantori [10]. After this event takes place, an entire new region of phase space becomes accessible to the exploration by the chaotic orbits. The decay exponent z drops drastically after

this point. A particularly interesting finding we report in this paper is that after the breakup of the outermost KAM surfaces surrounding the central island, another time scale $t_2 > t_1$ becomes important for the system. For particles that have escaped in the time interval $t_1 < t < t_2$, their trajectories lie entirely outside the newly created Cantori. Therefore, the exponent z measured over this intermediate interval is still roughly the same as that before the breakup of the corresponding KAM surfaces. The particles that stay longer than $t = t_2$, however, will explore the region enclosed by the newly created Cantori, thereby causing the exponent z to be markedly smaller than the one measured over the interval $t_1 < t < t_2$. Thus the curve $N(t)$ vs t exhibits two scaling regions with different decay exponents [11]. The time scale where this crossover takes place coincides with the typical time for a chaotic trajectory to penetrate the newly created Cantori.

This consideration can be repeatedly applied as the parameter further increases, thereby explaining the fluctuations displayed by the exponent z. As the system approaches hyperbolicity, the interval $0 < t < t_1$ becomes larger and larger reflecting the fact that the island structures in phase space become less and less significant. In the limit, we have $t_1 \to \infty$, and the system becomes completely hyperbolic. It should be pointed out that due to the limited range of numerical and experimental resolution and the observation time, the observational hyperbolicity, as signified by exponential decay in survival probability, will effectively set in earlier than the mathematically defined hyperbolicity.

A crossover between two algebraic decay regimes was also observed in a one-dimensional model of kicked hydrogen Rydberg atoms [12]. Again, the dynamics can be classified into three regions: (i) $0 \le t < t_1$, (ii) $t_1 \le t < t_2$, and (iii) $t > t_2$. While the decay in region (i) is nongeneric, two different decay exponents are observed in regions (ii) and (iii). The algebraic decay in region (iii) is due to the stickiness effect discussed above. The algebraic decay in region (ii), however, is due to a completely different decay mechanism which results in an algebraic decay in the absence of KAM islands [12].

It is a generally acknowledged notion that the algebraic decay in the presence of KAM surfaces should be a universal phenomenon with a single exponent. This notion is partly derived from the numerical works of Karney [1] and Chirikov and Shepelyansky [2]. In our opinion this may indeed be the case given the hierarchical island structure in phase space. But to attain such a universal exponent one needs a prohibitively long time to perform the needed numerical calculations. In the case of actual experiments the required long period of observation time becomes even more unrealistic. On the other hand, the algebraic decay behavior itself is found to occur on relatively short time scales. The value of the decay exponent measured over the time interval accessible to numerical experiments is influenced by the presence of dominant island structures. In this regard the variations of the exponent can, in fact, be utilized to reflect the major qualitative changes in the system. For this reason we believe that the phenomena occurring on short time scales, such as these investigated in this paper, should be given appropriate emphasis and considerations.

Finally we remark that parallel situations occur in systems with more than two degrees of freedom. In such systems a typical particle wanders in a well-defined phase-space region for a stretch of time before it hops to the next region along the Arnol'd web. This characteristic behavior is thought to underlie the observed crossover phenomena in the decay dynamics.

The organization of this paper is as follows. In Sec. II we introduce our model system and demonstrate that this system can exhibit nonhyperbolic chaotic scattering. In Sec. III we present our main numerical results establishing the theoretical picture depicted above. We conclude this paper in Sec. IV.

II. THE MODEL SYSTEM AND BIFURCATION TO CHAOTIC SCATTERING

The model system we use in this paper is a two-dimensional area-preserving map derived from a scattering problem. The scattering problem in this case consists of a point particle being scattered by an infinite array of nonoverlapping, elastic scatterers (Fig. 1) [13]. These scatterers are placed in the plane at constant intervals D along the y axis and each scatterer is represented by a circular potential $V(r)$ that vanishes for $r > R$ with $R < D/2$ (nonoverlapping condition). In the present study we choose $V(r)$ to be an attractive potential, i.e., $V(r) < 0$. If $V(r)$ is repulsive, only trivial invariant orbits can be formed in the potential region, thus rendering the system inept of displaying intricate dynamics.

The nonoverlapping condition entails that the particle trajectory is a straight line in the region between potential wells and suffers a deflection when the particle enters some scatterer. Let $\Theta(l)$ be the deflection angle of the particle trajectory caused by an individual scatterer. It can be argued that $\Theta(l)$ is a monotonically decreasing

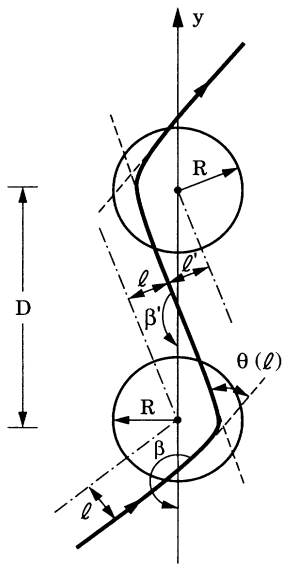

FIG. 1. The system of an infinite array of nonoverlapping, circular potentials.

function of the angular momentum l (at least near $l=0$). Assume that the particle mass is unity, then due to the finite range of each scatterer, $\Theta(l)=0$ for $l>l_{\max}=uR$, where u is the particle velocity (constant) during free motion. For a particle moving towards any of the scatterers with an angular momentum l and velocity $\mathbf{u}$, its new velocity $\mathbf{u}'$ after the scattering has the same magnitude as $\mathbf{u}$ but assumes a different direction. Let β and β' be the angles that $\mathbf{u}$ and $\mathbf{u}'$ make with respect to the negative y axis, measured counterclockwise. Then from Fig. 1 we have

$$\beta'=\beta+\Theta(l) . \tag{2}$$

Note that $\Theta(l)<0$ for $l>0$. Now the particle may either collide with the scatterer above (if $u_y'=-u\cos\beta'>0$) or with the scatterer below (if $u_y'<0$). In either case, the scattering is determined by the value of the angular momentum relative to the new scatterer which we denote by l'. Simple geometry shows that l' can be expressed as

$$l'=l+(Du)\mathrm{sgn}(\cos\beta')\sin\beta' . \tag{3}$$

Clearly the next scattering takes place only if $|l'|<l_{\max}$. Otherwise the particle will continue to move along a straight-line trajectory leaving the array of scatterers and will never return. Such particles will be regarded as having escaped in the subsequent discussions.

Symbolically, the two-dimensional map Eqs. (2) and (3) can be represented as

$$(\beta',l')=M(\beta,l) . \tag{4}$$

Phase space for M is defined by the domain $[0,2\pi)\times[-l_{\max},l_{\max}]$, which is a cylinder. [Here we have used the property that β is an angular variable, thus Eq. (2) can be considered as taking place on a circle.] It can be easily verified that M is area preserving.

To examine the evolution of the system shown in Fig. 1 we first note that, in the absence of the scatterer array [i.e., $V(r)=0$], no scattering takes place and particles simply travel along straight-line trajectories. On the other hand, the numerical evidence we present in the next section reveals an abundance of chaotic motion when $V(r)\neq 0$. Thus a natural question arises: How does chaos come about in this system? More specifically, setting V_0 as the parameter denoting the depth of the potential well $V(r)$, what are the typical sequences of events ("route") that occur as V_0 is increased from $V_0=0$ to a value where the scattering is chaotic? This is the question we address in the remainder of this section.

For a given physical potential $V(r)$, the deflection angle $\Theta(l)$ is likely to be a complicated function of l (see Sec. III). But, as indicated earlier, physical considerations require that $\Theta(l)$ is a monotonically decreasing function of l for values of l near $l=0$, and $\Theta(0)=0$. Thus for the purpose below we assume that $\Theta(l)=-kl$, where k is a nonnegative constant measuring the average slope of the monotonic portion of the $\Theta(l)$ vs l curve [13]. The two-dimensional map Eqs. (2) and (3) then becomes

$$\beta'=\beta-kl , \tag{5}$$

$$l'=l+(Du)\mathrm{sgn}[\cos(\beta-kl)]\sin(\beta-kl) . \tag{6}$$

This map has fixed points at $(\beta,l)=(0,0)$ and $(\beta,l)=(\pi,0)$, corresponding to orbits traveling along the negative- and positive-y axis, respectively. Due to the symmetry of the system we only need to analyze the linear stability for one of the fixed points, say $(\pi,0)$. Near $(\pi,0)$ the linearized mapping reads

$$\delta\beta'=\delta\beta-k\delta l , \tag{7}$$

$$\delta l'=Du\,\delta\beta+(1-Duk)\delta l . \tag{8}$$

The eigenvalues of this linear mapping are

$$\lambda_{\pm}=[(2-Duk)\pm(D^2u^2k^2-4Duk)^{1/2}]/2 . \tag{9}$$

When $k=0$, corresponding to $V(r)=0$ in the potential, we have $\lambda_{\pm}=1$. For $0<k<4/Du$, however, the eigenvalues $\lambda_{\pm}$ are complex and the fixed point is elliptic. Rigorous mathematical work due to Robinson [14], Newhouse [15], and Zehnder [16] reveals that, for nonintegrable systems, an elliptic fixed point is surrounded by layers of quasiperiodic orbits, other elliptic points, and most importantly, hyperbolic points whose stable and unstable manifolds form intricate homoclinic tangles (indicating the existence of chaotic invariant sets). In this sense, the transition to chaos occurs as soon as k becomes nonzero. In physical terms, chaotic scattering takes place immediately after we introduce an array of attractive potentials in the plane, regardless of the depth of each individual potential. Figures 2(a) and 2(b) schematically illustrate the above consideration. When $k=0$ the fixed point is the only component of the invariant set [Fig. 2(a)]. Figure 2(b) shows the fixed point and the associated KAM tori for k slightly above zero. In this case the chaotic regions are exponentially small and they exist between and outside the KAM tori. It is worth noting that this route to

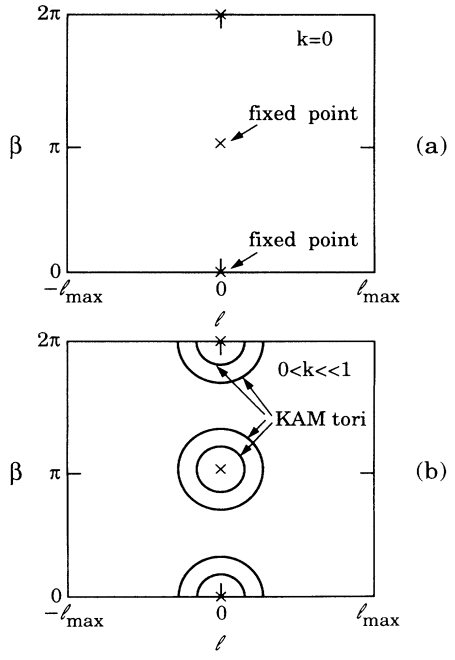

FIG. 2. Schematic illustration of the phase-space structure for (a) $k=0$, and (b) $0<k\ll 1$.

chaotic scattering is qualitatively different from the ones studied in the literature [17,18].

Beyond the initial bifurcation to chaos, phase space contains a mixture of KAM surfaces and chaotic components. Further increment of k leads the system to complete hyperbolic dynamics [13].

III. NUMERICAL RESULTS ON PARTICLE-DECAY DYNAMICS

In this section we present our main results establishing the mechanism underlying the dependence of the decay exponent on system parameters. For concreteness, we choose $V(r)$ to be a quadratic potential in the following form:

$$V(r)=-V_0\left[1-\left[\frac{r}{R}\right]^2\right] \quad \text{for } r\le R\ , \tag{10}$$

and $V(r)=0$ for $r>R$, where $V_0\ge 0$ measures the depth of the potential well. Using simple classical mechanics we obtain for the deflection angle,

$$\Theta(l)=2\sin^{-1}\left[\frac{l}{\sqrt{2E}R}\right]-\frac{l}{|l|}\left[\frac{\pi}{2}+\sin^{-1}\left[\frac{l^2/R^2-(E+V_0)}{[(E+V_0)^2-2l^2V_0/R^2]^{1/2}}\right]\right], \tag{11}$$

where E is the particle energy and the particle mass is chosen to be 1. In our subsequent calculations, we fix all the parameters in Eq. (11): $V_0=0.2$, $E=0.5$, and $R=1.0$ (so $l_{\max}=1$), and use the distance D between adjacent potentials as the control parameter. For small D values, the map Eqs. (2) and (3), with $\Theta(l)$ defined by Eq. (11), displays a mixture of regular motion on KAM surfaces and chaotic motion between these surfaces. For larger values of D, we did not find any KAM surfaces and particles appear to escape from the scattering region exponentially. Below we restrict our attention to the former range of D values.

To study the escape of particles, we proceed as follows. First we choose a subregion in the chaotic region which apparently does not intersect any KAM surfaces. We then initialize $N(0)$ particles uniformly in that subregion, and count the number of particles $N(t)$ that have not yet escaped the system at time t. From these data we extract the algebraic decay behavior by plotting $\log_{10}N(t)$ vs $\log_{10}t$. It can be seen that for $D=3.7$, the log-log plot shown in Fig. 3. is reasonably well fit by a straight line that extends over a few decades. The slope of the straight-line fit yields the decay exponent which, for the case in Fig. 3, is $z\approx 1.32$. The initial conditions used to generate Fig. 3 are placed at the lattice sites of a 2000×2000 uniform grid superposed on the subregion: $3.25\le\beta\le 3.30$ and $0.95\le l\le 1.00$.

As the parameter D varies, the decay exponent z fluctuates as shown in Fig. 4. In what follows we carry out a sequence of numerical experiments addressing the origin of this fluctuation. More specifically, we examine the phase-space structure and its associated dynamics for two pairs of D values, $D_1=3.60, D_2=3.62$, and $D_3=3.70, D_4=3.72$, respectively (see Fig. 4). Their corresponding decay exponents are denoted by z_1, z_2, z_3, and z_4, respectively. For the first pair of D values we have $z_2>z_1$, while for the second pair we have $z_4<z_3$. Thus, for increasing D values, the decay exponents increase for the first pair of D values. They decrease for the second pair. This is the reason for choosing the particular D values quoted above.

The phase-space structures corresponding to the first pair of D values, D_1 and D_2, are shown in Figs. 5(a) and 5(b), where we uniformly choose 144 initial conditions in the region $3.1<\beta<3.6$ and $0.87<l<0.92$. (Note that only parts of the phase space are shown in the figure highlighting the regions relevant to our discussion.) Some of the initial conditions lead to trajectories that lie on KAM surfaces, while others wander in the region of chaos. We have chosen to plot only the trajectories on the KAM surfaces. A noticeable feature common to both parameter values is that phase space is divided into two distinct regions by KAM surfaces. While the region denoted by B is enclosed within the KAM surfaces, the other region, denoted by A, lies outside the surfaces. As a result of this space partitioning, particles launched from outside visit only region A before they exit the potential. Region B in this case plays the role of the central island in our model consideration (see Sec. I). The particle-decay dynamics for both D_1 and D_2 is thus determined by the structures present in region A. As D increases from D_1 to D_2, the boundary between the two regions deforms slightly but otherwise remains essentially intact. In contrast, the area occupied by islands undergoes reduction from Fig. 5(a) to 5(b). The effect of this reduction is further demonstrated by plotting in its entirety the connected chaotic component in region A. This can be done, for bounded systems, by plotting a long

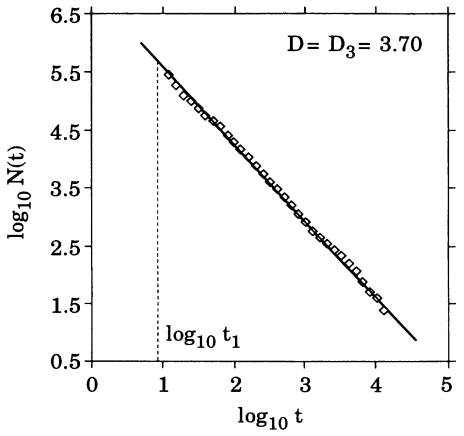

FIG. 3. $\log_{10}N(t)$ vs $\log_{10}t$ plot for $D=3.70$.

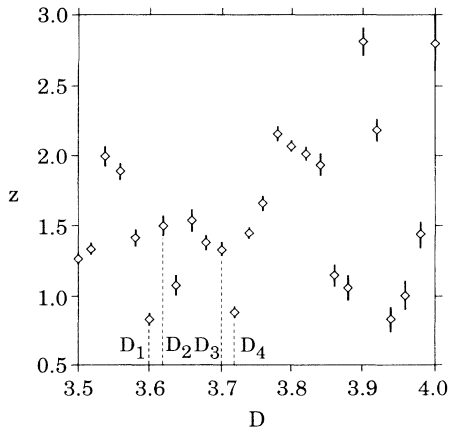

FIG. 4. Algebraic-decay exponent z as a function of the parameter D for $3.5 \leq D \leq 4.0$.

stretch of a chaotic trajectory. In the present system, however, such a simple procedure is inadequate because a typical trajectory exits the region before it traverses a substantial portion of the chaotic set. A possible remedy is to plot collectively the trajectories of many initial conditions. In our experiments we prefer another more elegant approach to obtain the unstable chaotic set. In this approach we make use of an orbit-tracing technique

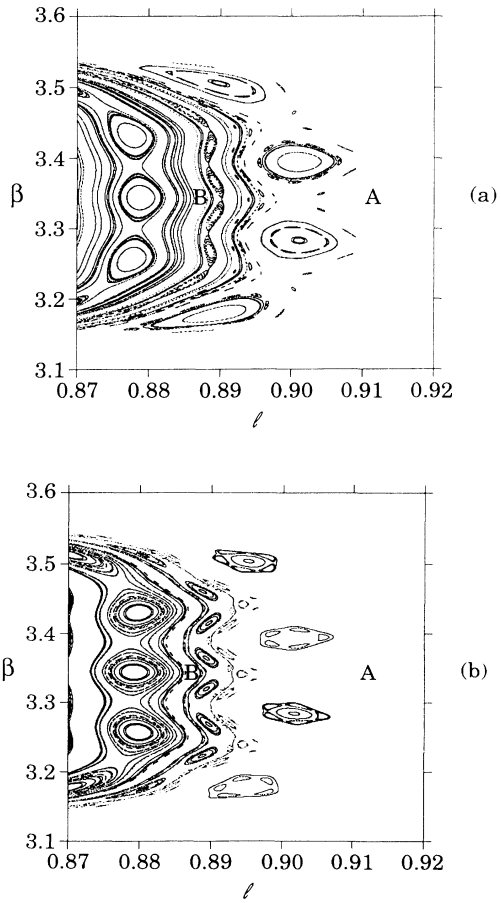

FIG. 5. Phase-space plots for (a) $D_1 = 3.60$ and (b) $D_2 = 3.62$.

called the proper interior maximum (PIM) -triple method [19]. The application of this method yields an arbitrarily long transitive orbit which approximates the chaotic set. Its basic steps are as follows. First we pick a long line segment in the chaotic region and uniformly sprinkle N points, $\mathbf{x}_i = (\theta_i, I_i)$, $i = 1,2,\ldots,N$, on the segment. Next we evolve those N particles under the scattering dynamics and calculate a delay time (the number of iterates a particle survives before escaping the scattering region) for each particle. In general a maximum delay time is attained by some point $\mathbf{x}_m$ in the interior of the initial segment. Around this point we form a new refined interval: $(\mathbf{x}_{m-1}, \mathbf{x}_{m+1})$. Sprinkle again N points on this new line segment and repeat the step above to obtain an even finer interval. Iterate the procedure until we get a line segment whose length is less than a predetermined value, say 10^{-9}. We call this process a "refinement procedure" and such a line segment with length less than 10^{-9} is called a "refined line segment." The middle point of this refined line segment then lies approximately on the stable manifold of the chaotic set. To get a numerical trajectory, we simply iterate forward the refined line segment under the dynamics. But due to the sensitivity to initial conditions, the length of the line segment grows exponentially with time. Therefore we need to stop the iteration when the length exceeds 10^{-9}, and perform the refinement procedure again to get a new refined segment. Hence, after an initial transient, the subsequent iterates of the middle point in the refined line segment shadows a transitive orbit on the chaotic invariant set. Sometimes it may so happen that the initial line segment intersects some KAM islands. In this case, the delay time for the point inside the island is infinite. To avoid this situation we set a critical time, say 10 000 iterations. If the delay time of a given point exceeds this critical time, we regard the particle as being inside some KAM island and discard the point consequently. Figures 6(a) and 6(b) display two long trajectories generated by the PIM-triple method for D_1 and D_2. Evidently the sum of blank pockets in region A, representing areas occupied by islands, is markedly smaller in Fig. 6(b) than that in Fig. 6(a). The implication in physical terms is that, on the average, particles exit the potential faster for $D_2 = 3.62$ than for $D_1 = 3.60$, thereby furnishing an explanation to the observed relationship $z_2 > z_1$. Note that if the experiments were to be performed for an infinitely long time the algebraic decay may yield an overall exponent which is the same for both parameter values.

We now turn to the second pair of D values, D_3, and D_4. For $D = D_4$, the decay exponent z attains a local minimum: $z_4 \approx 0.88$ (Fig. 4). The phase-space plots for D_3 and D_4 show drastic differences [Figs. 7(a) and 7(b)]. In particular, we note that while the two regions A and B in Fig. 7(a) are still visibly separated by KAM surfaces, the boundary between the two regions in Fig. 7(b) appears to have been destroyed. This situation entails that the chaotic component previously enclosed in region B is now accessible to the exploration of particles initialized in region A. In geometrical terms, the two chaotic regions lying on different sides of the KAM surfaces have been combined into a single connected chaotic set. To

prove this latter point we again make use of the PIM-triple method. The transitive orbits generated in this case are shown in Figs. 8(a) and 8(b), for D_3 and D_4, respectively. A close comparison with Figs. 7(a) and 7(b) confirms that the connected chaotic set at D_4 encompasses the region enclosed within region B at D_3.

It is known that Cantori, immediately after the breakup of KAM surfaces, serve as effective barriers to particle transport [10]. The typical time for a particle to penetrate the Cantori thus constitutes a new time scale in the system which we denote by t_2. The presence of this new time scale leads to observable consequences which we shall discuss below. For particles that exit the potential in time less than $t=t_2$, the corresponding trajectories lie entirely outside the newly created Cantori. This implies that the exponent measured over the time interval $t_1<t<t_2$ should be roughly the same as that before the breakup of KAM surfaces. Particles that stay longer than $t=t_2$, however, are likely to penetrate the Cantori and explore the chaotic component previously enclosed within the KAM surfaces. For these particles their trajectories encounter additional KAM island chains before they finally exit. Reflected in the decay dynamics this corresponds to a slower escape process, thus a smaller decay exponent measured over the interval $t>t_2$. The numerical results for D_3 and D_4 are shown in Figs. 3 and 9, respectively. There are clearly two regions of scaling behavior in Fig. 9. The exponent measured over the first interval of scaling behavior $t<t_2$ is $z\approx 1.27$, while the exponent measured over the remaining interval $t>t_2$ is $z\approx 0.88$. This confirms the theoretical consideration given above. We note that the latter value of z is what we use in Fig. 4. The crossover time $t=t_2$ in Fig. 9 is roughly 1200 iterates. As indicated, this time represents the number of iterates for a typical trajectory to penetrate the Cantori. To demonstrate this point we plot the trajectories for two sets of judiciously chosen initial conditions. One set yields trajectories which escape the potential before $t=t_2$. The other leads to orbits that stay longer than $t=t_2$. Figures 10(a) and 10(b) show the respective trajectories. One sees that the conclusion alluded to is self-evident.

In summary, we have shown that the number of surviving particles as a function of time decays algebraically for our nonhyperbolic chaotic scattering system. The decay exponent z measured over time intervals accessible to numerical experiments is influenced by the total area occupied by KAM island chains embedded in a chaotic com-

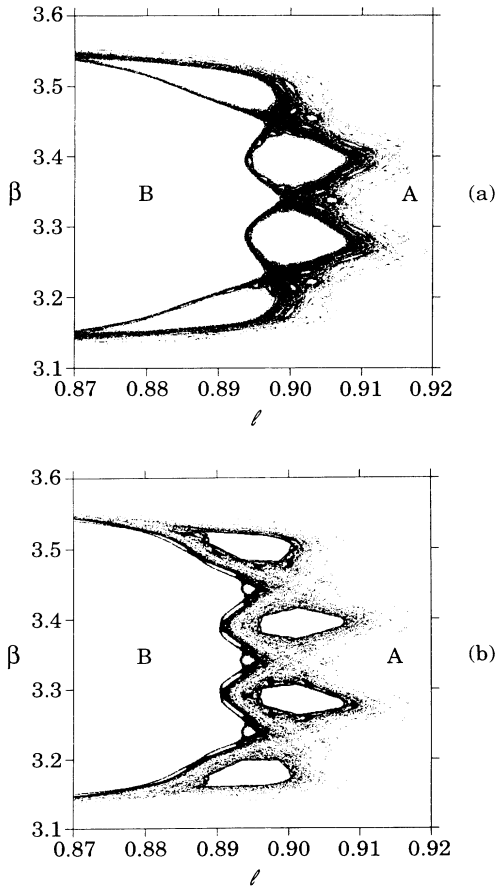

FIG. 6. PIM-triple trajectories for (a) $D_1=3.60$ and (b) $D_2=3.62$.

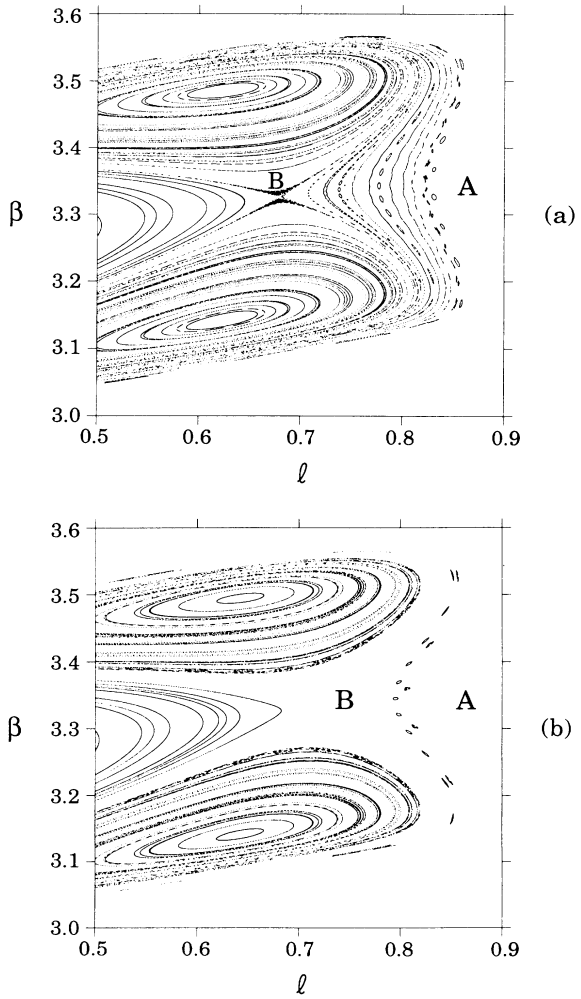

FIG. 7. Phase-space plots for (a) $D_3=3.70$ and (b) $D_4=3.72$.

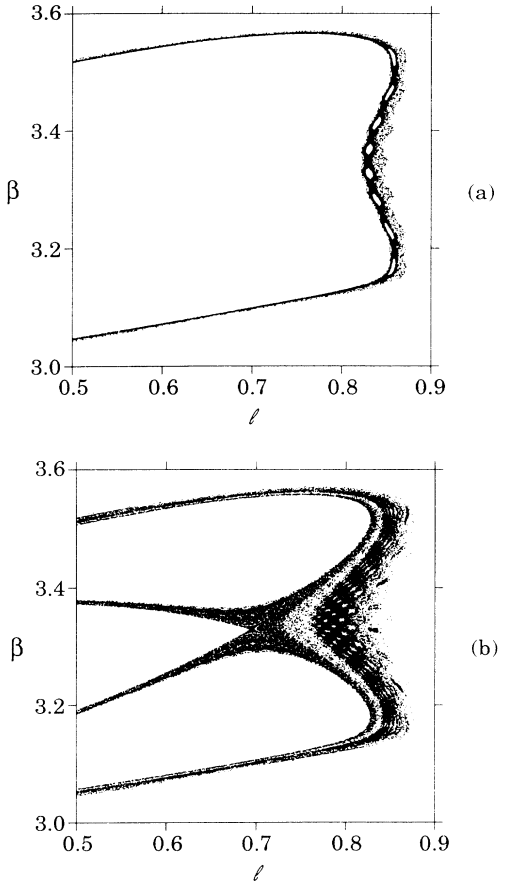

FIG. 8. PIM-triple trajectories for (a) $D_3=3.70$ and (b) $D_4=3.72$.

ponent that is accessible to the scattering trajectory. The area occupied by the island chains is, in turn, determined by the creation and destruction of KAM surfaces. When phase space undergoes a major metamorphosis [11], which for our case is exemplified by the destruction of the KAM surfaces enclosing a central island and subsequent exposure of a new layer of KAM islands, the particle-decay curve exhibits two regions of scaling behavior. The interpretation afforded for this crossover phenomenon

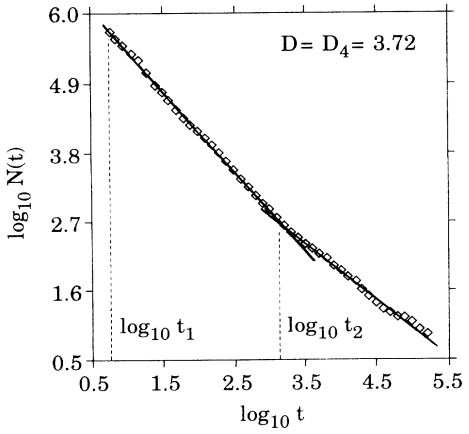

FIG. 9. $\log_{10}N(t)$ vs $\log_{10}t$ plot for $D_4=3.72$.

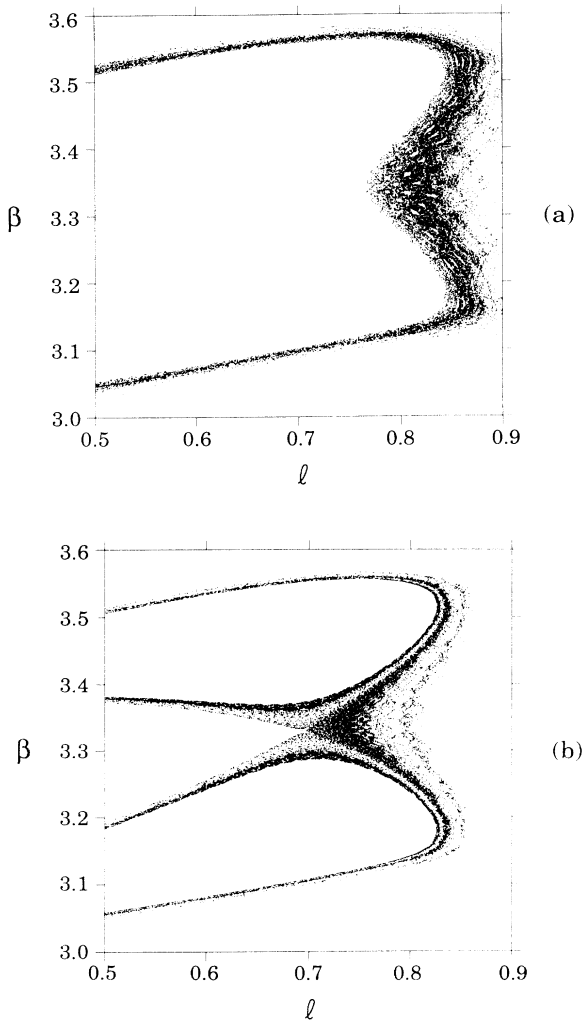

FIG. 10. Two-particle trajectories corresponding to escape time (a) $t<t_2$ and (b) $t>t_2$ ($D=3.72$).

suggests that, due to the continual nature of KAM surface breakup on all scales, one should observe multiple crossovers at different time scales. This conforms with Fig. 6 in Ref. [1] which is a result of an extremely long numerical simulation. But with the limited time frame within which a typical experiment is carried out, only crossover associated with major changes in phase space falls into the window of observability. As a parameter varies, along with island destructions there are also island creations through saddle-center bifurcations. In most cases, however, the sizes of the islands accompanying the center are insignificant and thus its impact is only felt on time scales beyond typical experimental resolution.

Finally we remark that systems with more than two degrees of freedom depart from low-dimensional systems in that the energy surface is no longer isolated into regions enclosed by KAM surfaces. The chaotic set in this case forms a single integrated component on which a typical particle can execute Arnol'd diffusion. If the energy surface is unbounded, it is found that the particle decay obeys algebraic laws [5]. Using a three-dimensional generalization of the potential in Fig. 1, we have observed

features of the decay dynamics analogous to what we see in low dimensions. In particular, the characteristic behavior of Arnol'd diffusion in which a particle hops for one well-defined region in phase space into another closely resembles the penetration of Cantori in two-dimensional systems. This apparently leads to multiple decay exponents measured over short intervals of time. A detailed exposition of higher-dimensional dynamics will be presented elsewhere.

IV. CONCLUSIONS

The results of this study show that a metamorphosis in phase space exemplified by the destruction of KAM surfaces and subsequent exposure of a new layer of KAM islands may manifest itself through variations in the decay exponent. Conversely, this relationship can also be used to interpret unexpected findings in physical experiments. One of such examples is the study reported in Ref. [11] where the authors consider a theoretical model of microwave ionization of hydrogen Rydberg atoms. Their results indicate that, contrary to naive physical intuition, the ionization rate, analogous to the decay exponent z in our case, is not a monotonically increasing function of the field strength. In many instances the increment of the field strength actually leads to a decline of the ionization rate. The reasons behind the finding are precisely what we report in this paper, namely, the complicated metamorphosis patterns in phase space.

Finally we stress that the phenomena examined in this work mainly occur on time scales far shorter than that required for observing universal dynamics. Nevertheless, as the results show, this nonuniversal behavior can in fact be utilized to reflect qualitative changes in the system. In this regard, we submit that the phenomenology related to our observability is an important problem which warrants further consideration.

ACKNOWLEDGMENTS

This work was supported by the Department of Energy (Scientific Computing Staff, Office of Energy Research). R.B. is grateful for financial support by the Deutsche Forschungsgemeinschaft.

[1] C. F. F. Karney, Physica D **8**, 360 (1983).
[2] B. V. Chirikov and D. L. Shepelyansky, Physica D **13**, 394 (1984).
[3] P. Grassberger and H. Kantz, Phys. Lett. A **113**, 167 (1985).
[4] H. Kantz and P. Grassberger, Phys. Lett. A **123**, 437 (1987).
[5] M. Ding, T. Bountis, and E. Ott, Phys. Lett. A **151**, 395 (1990).
[6] F. Vivaldi, A. Casati, and I. Guarneri, Phys. Rev. Lett. **51**, 727 (1983).
[7] K.-C. Lee, Phys. Rev. Lett. **60**, 1991 (1988).
[8] J. D. Hanson, J. Cary, and J. D. Meiss, J. Stat. Phys. **39**, 327 (1985).
[9] J. D. Meiss and E. Ott, Phys. Rev. Lett. **55**, 2741 (1985); Physica D **20**, 387 (1986).
[10] R. S. MacKay, J. D. Meiss, and I. C. Percival, Phys. Rev. Lett. **52**, 697 (1984).
[11] Y. C. Lai, C. Grebogi, R. Blümel, and M. Ding, Phys. Rev. A **45**, 8284 (1992).
[12] C. F. Hillermeier, R. Blümel, and U. Smilansky, Phys. Rev. A **45**, 3486 (1992).
[13] G. Troll and U. Smilansky, Physica D **35**, 34 (1989).
[14] R. C. Robinson, Am. J. Math. **102**, 562 (1970).
[15] S. E. Newhouse, Am. J. Math. **99**, 1061 (1975).
[16] E. Zehnder, Commun. Pure Appl. Math. **26**, 131 (1973).
[17] S. Bleher, E. Ott, and C. Grebogi, Phys. Rev. Lett. **63**, 919 (1989); S.Bleher, C. Grebogi, and E. Ott, Physica D **46**, 87 (1990).
[18] M. Ding, C. Grebogi, E. Ott, and J. A. Yorke, Phys. Rev. A **42**, 7025 (1990).
[19] H. E. Nusse and J. A. Yorke, Physica D **36**, 137 (1989).

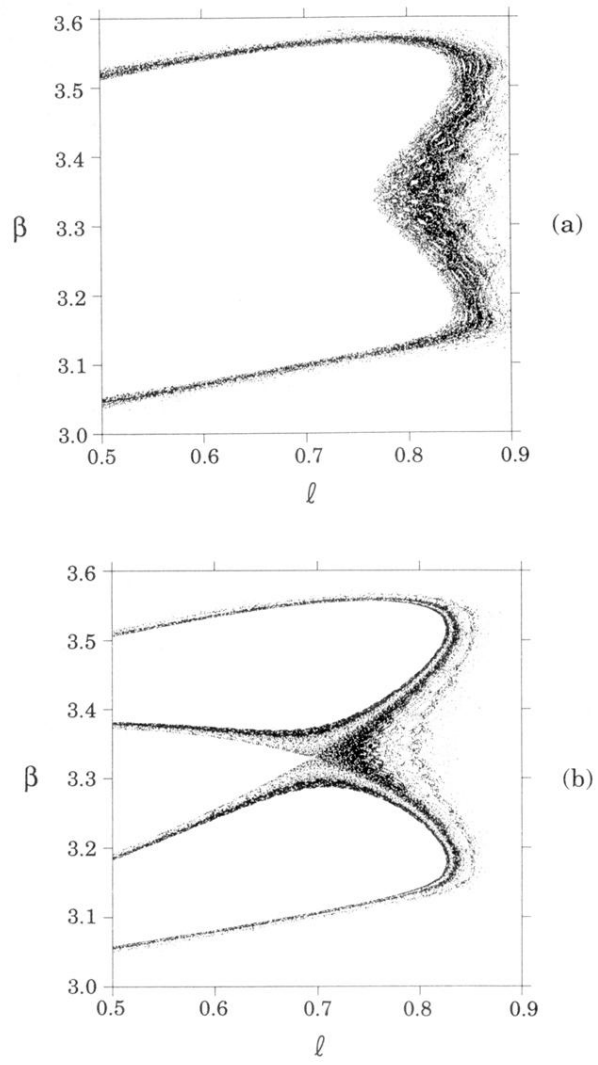

FIG. 10. Two-particle trajectories corresponding to escape time (a) $t < t_2$ and (b) $t > t_2$ ($D = 3.72$).

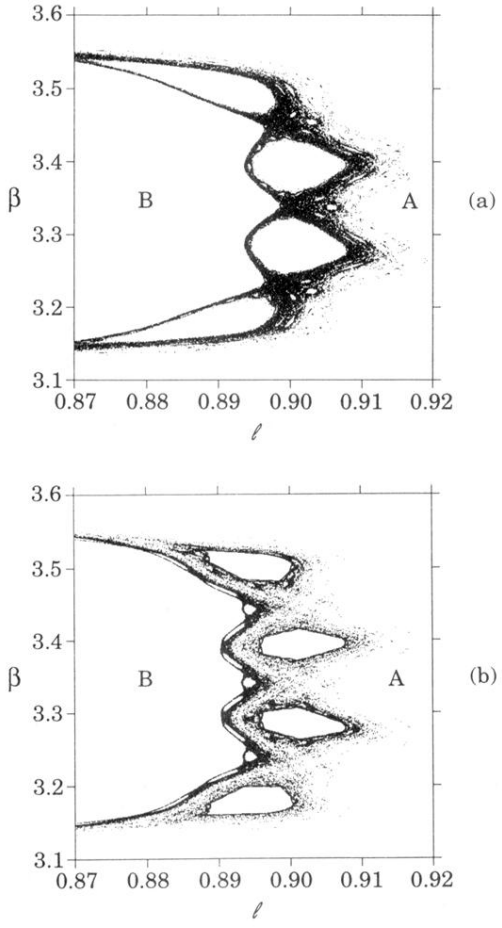

FIG. 6. PIM-triple trajectories for (a) $D_1 = 3.60$ and (b) $D_2 = 3.62$.

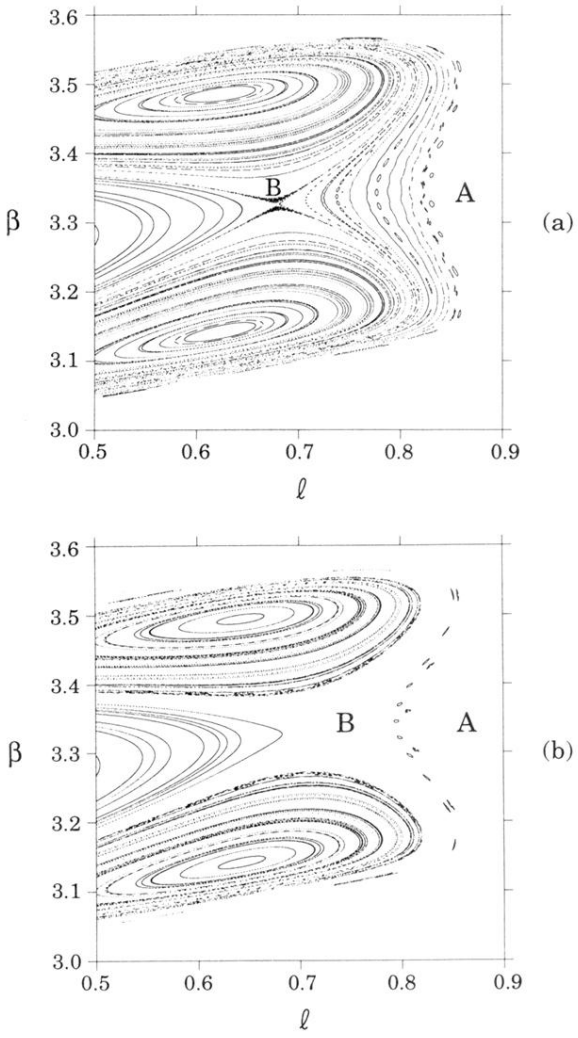

FIG. 7. Phase-space plots for (a) $D_3 = 3.70$ and (b) $D_4 = 3.72$.

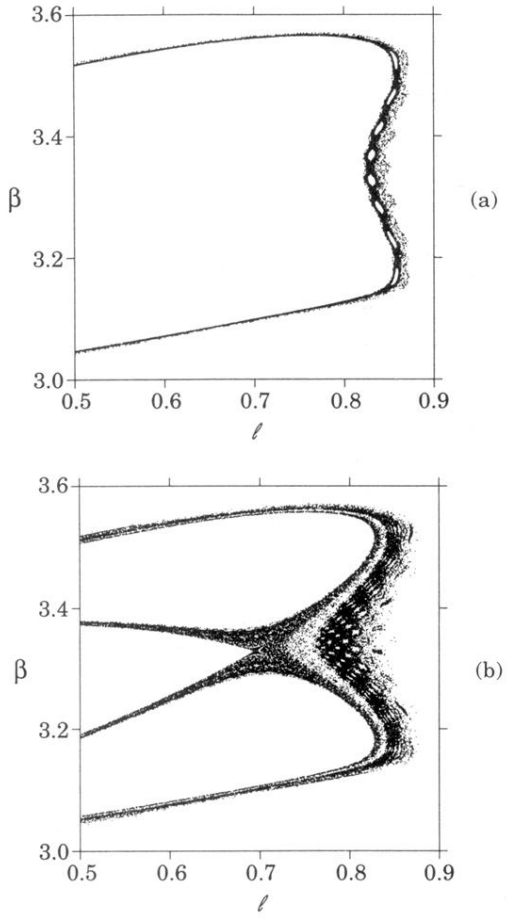

FIG. 8. PIM-triple trajectories for (a) $D_3 = 3.70$ and (b) $D_4 = 3.72$.